

Erbium-implanted silica microsphere laser

J. Kalkman^{a,*}, A. Polman^a, T.J. Kippenberg^b, K.J. Vahala^b, Mark. L. Brongersma^c

^a FOM Institute for Atomic and Molecular Physics, Kruislaan 407, 1098 SJ, Amsterdam, The Netherlands

^b Department of Applied Physics, California Institute of Technology, Pasadena, CA 91125, USA

^c Department of Material Science and Engineering, Stanford University, Stanford, CA 94305, USA

Available online 7 October 2005

Abstract

Spherical silica optical microresonators were doped with erbium ions by ion implantation at energies of 925 keV and 2.05 MeV using a rotating stage. After thermal annealing at 800 °C, light was coupled into the microsphere using a tapered optical fiber. An optical quality factor as high as 1.9×10^7 was observed at $\lambda = 1450$ nm, corresponding to a modal loss of only 0.01 dB/cm. When pumped at 1450 nm, multi-mode lasing around 1570 nm is observed at a threshold between 150 and 250 μ W depending on the overlap between mode and Er distribution. This work demonstrates the compatibility of ion implantation and microresonator technology.

© 2005 Elsevier B.V. All rights reserved.

PACS: 42.55.Sa; 42.60.Da; 42.81.Qb; 85.40.Ry

Keywords: Microsphere; Laser; Erbium; Ion implantation

1. Introduction

Optical microcavities are now being studied over both a wide range of applications and geometries [1]. Of all optical microcavities, silica microspheres [2] exhibit the highest quality (Q) factors to date. Q factors of more than 10^9 can be obtained [3], corresponding to optical losses that are several orders of magnitude lower than typical losses in planar waveguide structures. Spherical microcavities are made of silica glass using melting and surface-tension induced smoothing. When doped with optically active erbium ions, these microspheres show lasing at the $^4I_{13/2} \rightarrow ^4I_{15/2}$ transition of Er^{3+} around 1.5 μm [4]. So far, lasing has been observed in microspheres that were homogeneously doped with Er. In this geometry, the low-intensity tails of the optical pump mode lead to incomplete pumping of certain erbium-doped regions that interact with the lasing mode. The resulting large absorption due to unexcited Er can increase the lasing threshold, and in-

duce pulsed-mode operation due to saturable absorption. To achieve lower thresholds and continuous-wave operation, it would be advantageous to fabricate structures where the Er distribution is tailored to the optical mode, with the peak Er concentration located at the peak of the mode distribution. One route to such an optimized profile involves coating the surface of a sphere with a thin layer of erbium-doped sol-gel [5]. In this paper we describe an alternative method using high-energy Er implantation. We demonstrate that very high Q factors ($>10^7$) can be achieved in ion-implanted microspheres and demonstrate low-threshold (150 μW) lasing operation.

2. Experimental

Silica microspheres were made by melting the end of a stripped standard telecommunication fiber (SMF 28) with a CO_2 laser ($\lambda = 10.6 \mu\text{m}$). After melting and solidification controlled by surface tension, a near-perfect spherical shape, with a radius of $\sim 22 \mu\text{m}$ was achieved (see inset in Fig. 1). The microsphere remained attached to the fiber stem, which was subsequently heated to induce a 90° bend,

* Corresponding author. Tel.: +31 20 608 1234; fax: +31 20 668 4106.
E-mail address: library@amolf.nl (J. Kalkman).

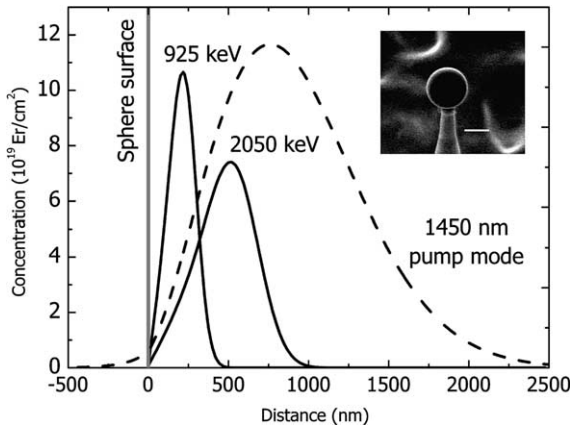


Fig. 1. Calculated Er implantation profiles for 22 μm -diameter silica microspheres implanted with 925 keV Er^+ ($7.2 \times 10^{15} \text{ cm}^{-2}$) and 2.05 MeV Er^{2+} ($1.1 \times 10^{16} \text{ cm}^{-2}$) using a rotating geometry. Measured ion ranges and straggles for planar samples were used as input. Also indicated is the 1450 nm pump mode profile (dashed line) for a 22 μm radius sphere. The inset shows an optical micrograph of a microsphere on the fiber stem (scale bar 50 μm).

enabling convenient attachment of the microresonator-stem assembly to a planar substrate with ceramic adhesive. Before further processing the optical Q factor was tested and values in excess of 10^8 were observed. The substrate was then mounted on a rotating stage, allowing homogeneous implantation of Er ions into the surface of the microsphere along the whole circumference. The rotation of the microsphere also prevents deformation of the sphere caused by the ion beam [6]. Erbium ions were generated using a sputter ion source in a 1 MV van de Graaff accelerator. The ion beam was electro-statically scanned through a $5 \times 5 \text{ mm}^2$ aperture, while the microsphere was slowly rotated around the stem axis. In this way homogeneous Er implantation distributions were obtained in the microsphere's equatorial plane. Two samples were made: 925 keV Er^+ implanted at a fluence of $7.2 \times 10^{15} \text{ cm}^{-2}$, and 2.05 MeV Er^{2+} implanted at a fluence of $1.1 \times 10^{16} \text{ cm}^{-2}$. Planar reference samples were implanted simultaneously, and then analyzed using Rutherford backscattering spectrometry. Gaussian depth profiles were observed in the planar sample, peaking at 265 (614) nm with a straggle of $\sigma = 71$ (142) nm for the 925 (2050) keV implant. Due to the spherical shape and rotation of the sample, the Er depth profile in the microresonator is substantially different from that of the planar reference sample. Fig. 1 shows the calculated Er depth profiles in the radial direction of the equatorial plane. When compared to the reference samples, both a reduced Er peak concentration and a reduced projected range were observed, with the 925 keV implant peaking at 226 nm (peak concentration $1.1 \times 10^{20} \text{ cm}^{-3}$ (0.16 at.%)), and the 2.05 MeV implant peaking at 501 nm (peak concentration $7.4 \times 10^{19} \text{ cm}^{-3}$ (0.12 at.%)).

Fig. 1 also shows the calculated depth distribution of the fundamental mode in a 22 μm -radius microsphere at $\lambda = 1450 \text{ nm}$, a typical pump wavelength. As can be seen,

the overlap between Er distribution and pump mode for the 2.05 MeV implant ($\Gamma_{2050} = 0.31$) is much larger than for the 925 keV implant ($\Gamma_{925} = 0.07$). Indeed, as aimed for in this experiment, negligible Er is present in the deeper tails of the mode beyond 1 μm depth. After implantation, the microspheres were annealed for 1 h at 800 $^\circ\text{C}$ in a vacuum oven to optically activate the Er ions [7]. The Er photoluminescence lifetime measured at $\lambda = 1535 \text{ nm}$ was 10–12 ms for both samples, typical for Er in silica at a concentration of $\sim 0.1 \text{ at.}\%$ [7].

3. Results and discussion

To measure the lasing characteristics of the Er-implanted microspheres, a tapered optical fiber was fabricated and coupled to the microsphere (see inset in Fig. 2). Details of the taper fabrication process and coupling geometry are described in [8]. The output from a

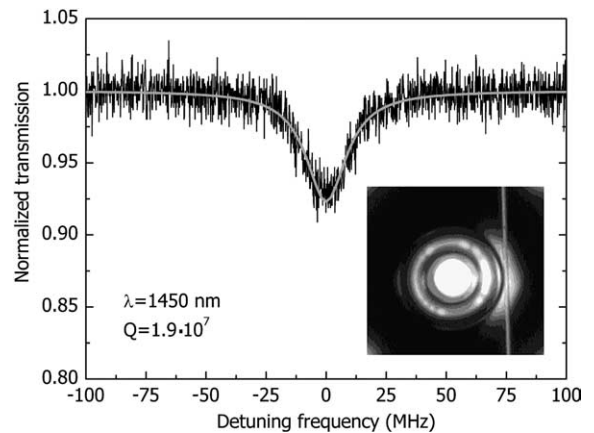


Fig. 2. Optical transmission spectrum around $\lambda = 1450 \text{ nm}$ measured in the under-coupled regime. Solid line shows a fit from which the quality factor ($Q = 1.9 \times 10^7$) was derived. The inset shows a top view of the fiber-microresonator coupling geometry.

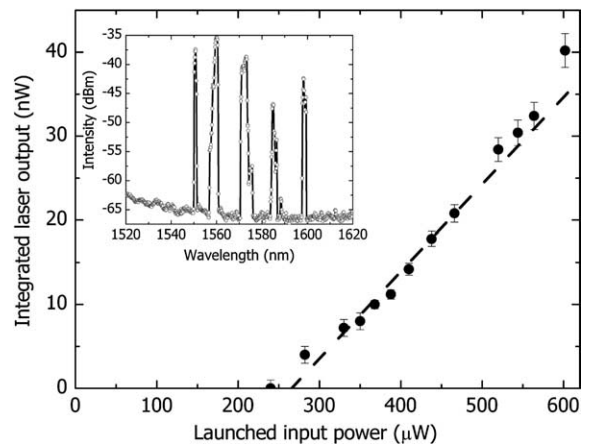


Fig. 3. Lasing output power integrated over all lasing lines plotted as a function of pump power at 1450 nm for a microcavity doped with 925 keV Er. A lasing threshold of 250 μW is observed. The inset shows a typical lasing spectrum.

tunable external-cavity diode laser operating around $1.5\ \mu\text{m}$ was coupled into the fiber, and the transmitted and reflected power were monitored at output and input ends. Lasing emission was collected through the tapered fiber and analyzed with an optical spectrum analyzer.

Fig. 2 shows the transmission spectrum around $\lambda = 1450\ \text{nm}$ for a tapered fiber positioned more than $1\ \mu\text{m}$ from the $2.05\ \text{MeV}$ implanted microsphere (i.e. in the under-coupled regime). By fitting the spectral shape of the resonance, an intrinsic Q factor of 1.9×10^7 was obtained. This value is similar to the Er-absorption related Q (calculated using the mode overlap determined from Fig. 1 and the Er absorption cross section $2 \times 10^{-22}\ \text{cm}^2$ at $1450\ \text{nm}$ [9]) and shows that cavity losses are dominated by Er absorption rather than intrinsic losses. Besides absorption, scattering centers can give rise to strong modal coupling and splitting of modes into doublets [10]. The absence of splitting indicates that ion implantation and subsequent thermal annealing does not create additional scattering. The obtained quality factor of 1.9×10^7 corresponds to a modal loss in the order of $0.01\ \text{dB/cm}$, which is quite well suited for many applications. This clearly shows that high-energy ion implantation, when combined with the proper thermal processing, is compatible with high- Q microcavity fabrication.

When pumped at a sufficiently high power, the Er-implanted microsphere exhibits lasing. The inset in Fig. 3 shows a lasing spectrum (launched pump power $> 1\ \text{mW}$) of the $925\ \text{keV}$ implanted sample taken at a relatively low optical resolution ($\Delta\lambda = 0.14\ \text{nm}$). Multimode lasing operation is observed at wavelengths slightly longer than the wavelength of the main Er transition. The latter is attributed to the lower Er absorption cross section at longer wavelengths, causing a reduced lasing threshold [11]. From the spectral spacing in the lasing spectrum a free spectral range of $12\ \text{nm}$ is derived, corresponding to a sphere radius of approximately $22\ \mu\text{m}$.

Fig. 3 shows, for the $925\ \text{keV}$ Er implanted sample, the output power, integrated over all lasing lines, as a function of input power launched into the input fiber. A linear increase of the output power is observed above a threshold of $250\ \mu\text{W}$. The slope efficiency measured under these coupling conditions is 1×10^{-4} . The conversion efficiency can be significantly increased by increasing the Er concentra-

tion [11]. Consequently, this will result in an increased lasing threshold. A similar measurement was performed for the $2.05\ \text{MeV}$ implanted sample, and a lasing threshold of $150\ \mu\text{W}$ was observed (data not shown). This lower threshold for the deeper implant is consistent with the better overlap between Er and mode profile, as shown in Fig. 1.

When operated at pump powers far above the $1.5\ \mu\text{m}$ lasing threshold, clear green emission from the microlaser was observed by the naked eye. Optical micrographs taken with a CCD camera sensitive in the visible are shown in Fig. 4 for the $2.05\ \text{MeV}$ Er implanted sample. The visible emission bands are attributed to transitions from the $^4\text{F}_{7/2}$ and $^2\text{H}_{11/2}$ levels to the ground state of Er^{3+} . These higher lying levels can be populated through a combination of cooperative up-conversion and excited state absorption transitions [12]. By changing the coupling conditions (e.g. taper–fiber distance) different spatial modes can be excited with different spatial upconversion emission patterns, as can be seen in Fig. 4(a)–(c). Whispering gallery modes are described by three mode numbers: angular (l), azimuthal (m), and radial (n). Fig. 4 shows a fundamental mode ($n = 1$) (a); a mode with two nodes in the polar direction, i.e. $l - m = 2$ (b); and a mode with a very high inclination, $l - m \gg 1$ (c). These data show that Er up-conversion emission can be used to provide detailed information on the mode structure in optical microcavities, an effect demonstrated earlier for planar waveguides [13]. This is particularly useful in geometries where the mode profile cannot be calculated analytically. Note that by using this technique of upconversion imaging a spatial imaging resolution for the infrared mode can be achieved that is well below the diffraction limit at the mode wavelength.

Finally, we note that the above work on ion-implanted resonators provided the inspiration for a subsequent project on Er ion implantation doping of toroidal microresonators on a Si chip. Er ions were implanted in thermal silica that was subsequently processed to form a disk on a Si post on a Si wafer. The disk was subsequently collapsed into a toroidal structure using a CO_2 laser annealing technique pioneered by Armani et al. [14]. When pumped at $1.48\ \mu\text{m}$ these structures show single mode lasing at $1.55\ \mu\text{m}$, at a threshold below $5\ \mu\text{W}$. More details on these measurements can be found in [11,15].

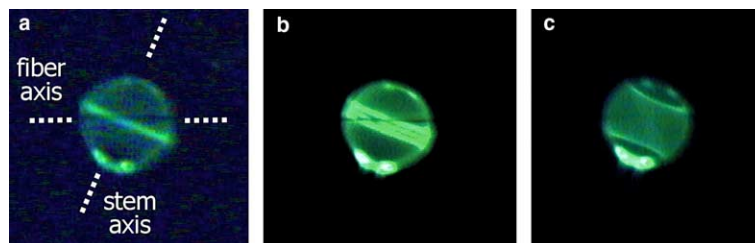


Fig. 4. Optical micrographs of an Er-implanted microsphere ($2.05\ \text{MeV}$) under lasing conditions. Green upconversion emission is imaged (printed in black and white). Directions of fiber axis and microsphere stem are indicated. Three different coupling conditions are used in images (a), (b) and (c), leading to distinctly different optical mode spatial distributions.

4. Conclusions

In summary, we have shown that high energy Er ion implantation (925 keV, 2.05 MeV) can be used to dope spherical optical microcavities with optically active Er ions with a depth distribution that matches well with the fundamental optical mode. When pumped at 1450 nm, lasing is observed, with a lowest launched pump power threshold of 150 μ W. This work also shows that high-energy ion implantation, in combination with thermal annealing, can lead to doped microcavities with very high Q ($>10^7$). These findings open up a new field of ion implantation/microresonator technology, as all ion beam materials synthesis techniques developed for planar films can now be applied to optical microresonator structures.

Acknowledgements

The Dutch part of this work is part of the research program of the “Stichting voor Fundamenteel Onderzoek der Materie (FOM)”, which is financially supported by the “Nederlandse organisatie voor Wetenschappelijk Onderzoek (NWO)”. The Caltech portion was supported by DARPA, NSF and the Lee Center.

References

- [1] K.J. Vahala, Nature 424 (2003) 839.
- [2] V.B. Braginsky, M.L. Gorodetsky, V.S. Ilchenko, Phys. Lett. A 137 (1989) 393.
- [3] D.W. Vernooy, V.S. Ilchenko, H. Mabuchi, E.W. Streed, H.J. Kimble, Opt. Lett. 23 (1998) 247.
- [4] M. Cai, O. Painter, K.J. Vahala, P.C. Sercel, Opt. Lett. 25 (2000) 1430.
- [5] L. Yang, K.J. Vahala, Opt. Lett. 28 (2003) 592.
- [6] E. Snoeks, A. van Blaaderen, C.M. van Kats, M.L. Brongersma, T. van Dillen, A. Polman, Adv. Mat. 12 (2000) 1511.
- [7] A. Polman, J. Appl. Phys. 82 (1997) 1.
- [8] S.M. Spillane, T.J. Kippenberg, O.J. Painter, K.J. Vahala, Phys. Rev. Lett. 91 (2003) 043902-1.
- [9] W.J. Miniscalco, J. Lightwave Technol. 9 (1991) 234.
- [10] T.J. Kippenberg, S.M. Spillane, K.J. Vahala, Opt. Lett. 27 (2002) 1669.
- [11] B. Min, T.J. Kippenberg, J. Kalkman, K.J. Vahala, A. Polman, Phys. Rev. A. 70 (2004) 033803.
- [12] G.N. van den Hoven, E. Snoeks, A. Polman, C. van Dam, J.W.M. van Uffelen, M.K. Smit, J. Appl. Phys. 79 (1996) 1258.
- [13] G.N. van den Hoven, A. Polman, C. van Dam, J.W.M. van Uffelen, M.K. Smit, Opt. Lett. 21 (1996) 576.
- [14] D.K. Armani, T.J. Kippenberg, S.M. Spillane, K.J. Vahala, Nature 421 (2003) 925.
- [15] A. Polman, B. Min, J. Kalkman, T. Kippenberg, K.J. Vahala, Appl. Phys. Lett. 84 (2004) 1037.